Journal of Cleaner Production 259 (2020) 120788

Contents lists available at ScienceDirect

Journal of Cleaner Production

journal homepage: www.elsevier.com/locate/jclepro

Bipolar membrane electrodialysis for energetically competitive ammonium removal and dissolved ammonia production

Niels van Linden [a, *], Giacomo L. Bandinu [a], David A. Vermaas [b, c], Henri Spanjers [a], Jules B. van Lier [a]

[a] Delft University of Technology, Faculty of Civil Engineering and Geosciences, Stevinweg 1, 2628 CN, Delft, the Netherlands
[b] Delft University of Technology, Faculty of Applied Sciences, Van der Maasweg 9, 2629 HZ, Delft, the Netherlands
[c] AquaBattery B.V, Lijnbaan 3C, 2352 CK, Leiderdorp, the Netherlands

ARTICLE INFO

Article history:
Received 5 November 2019
Received in revised form
28 January 2020
Accepted 26 February 2020
Available online 29 February 2020

Handling editor: Xin Tong

Keywords:
Water treatment
Ammonia recovery
Water dissociation
Current efficiency
Energy consumption

ABSTRACT

Removal of ammoniacal nitrogen from residual waters traditionally relies on energy-consuming biochemical processes, while more novel alternative strategies focus on the recovery of total ammoniacal nitrogen for the production of fertilisers or the generation of energy. The recovery of total ammoniacal nitrogen as gaseous ammonia is more effective at high ammonia concentrations in the liquid feed. Typically, chemicals are added to increase the solution pH, while

bipolar membrane electrodialysis can be used to convert salt solutions to acid and base solutions by using only electricity. In this study, we used bipolar membrane electrodialysis to remove ammonium from water and to simultaneously produce concentrated dissolved ammonia, without using chemicals. The energy consumption and current efficiency to transport ammonium from the diluate (the feed water) were assessed throughout sequencing batch experiments.

The total ammoniacal nitrogen removal efficiency for bipolar membrane electrodialysis ranged between 85 and 91% and the energy consumption was stable at 19 MJ·kg-N^{-1}, taking both electrochemical and pumping energy into account. The base pH increased from 7.8 to 9.8 and thetotal ammoniacal nitrogen concentration increased from 1.5 to 7.3 g L^{-1}, corresponding to a final ammonia concentration of 4.5 g L^{-1} in the base. Leakage of hydroxide, diffusion of dissolved ammonia and ionic species from the base to the diluate all contributed to a loss in current efficiency. Due to the increase in operational run time and concentration gradients throughout the sequencing batch experiments, the current efficiency decreased from 69 to 54%. We showed that

bipolar membrane electrodialysis can effectively be used to simultaneously remove ammonium from water and produce concentrated dissolved ammonia while avoiding the use of chemicals. Moreover, the energy consumption was competitive with that of the combination of electrodialysis and the addition of chemicals (22 MJ·kg-N^{-1}).

© 2020 The Authors. Published by Elsevier Ltd. This is an open access article under the CC BY-NC-ND license (http://creativecommons.org/licenses/by-nc-nd/4.0/).

1. Introduction

1.1. Emission of ammoniacal nitrogen to the environment

Ammonia (NH_3) is one of world's most-produced chemicals and is mainly used for the production of fertilisers. According to the review of Erisman et al. (2007), half of the produced NH_3 eventually ends up in the global environment and contributes to eutrophication and subsequent biodiversity loss. The direct discharge of domestic and industrial residual (waste) waters containing ammoniacal nitrogen largely contributes to the global nitrogen pollution.

1.2. Treatment of residual waters containing ammoniacal nitrogen

To limit the ammoniacal nitrogen emission to the aqueous environment, residual waters are treated before discharge. Ammoniacal nitrogen can be present in water in two forms, of which the distribution mainly depends on the temperature and pH of the water. The presence of ammoniacal nitrogen is therefore

* Corresponding author.
E-mail address: N.vanLinden@tudelft.nl (N. van Linden).

https://doi.org/10.1016/j.jclepro.2020.120788
0959-6526/© 2020 The Authors. Published by Elsevier Ltd. This is an open access article under the CC BY-NC-ND license (http://creativecommons.org/licenses/by-nc-nd/4.0/).

often described by the total ammoniacal nitrogen (TAN) concentration, which is the sum of both dissolved NH_3 and ammonium (NH_4^+). In residual waters, TAN is predominantly present as NH_4^+. Traditionally, NH_4^+ is removed by biochemical conversion of NH_4^+ to nitrogen gas by the energy-intensive nitrification-denitrification process. More recently, less energy-intensive concepts based on anammox processes are increasingly applied for residual waters with high TAN concentrations (>0.1 g L^{-1}) (Gonzalez-Martinez et al., 2018). However, in literature it is described that the application of nitrification-denitrification and anammox processes results in the generation and emission of harmful oxidised nitrogen species such as N_2O (Kampschreur et al., 2009).

1.3. Recovery of ammoniacal nitrogen from residual waters

Alternative TAN removal strategies aim to recover TAN as (raw material for) fertiliser from residual waters with high TAN concentrations, using mature technologies such as struvite precipitation and air stripping in combination with acid scrubbing (Mehta et al., 2015). However, these technologies depend heavily on the use of chemicals, which are typically produced elsewhere and need to be safely transported and stored. Moreover, (electrochemical) membrane technologies such as (bio-)electrochemical cells and electrodialysis (ED) are widely studied to recover TAN without use of chemicals as fertiliser from residual waters such as reject water and urine (Kuntke et al., 2018; Xie et al., 2016).

Besides the recovery of TAN as (raw material for) fertiliser, new strategies comprise the recovery of TAN from residual waters for the generation of electrical and thermal energy in a solid oxide fuel cell (SOFC) (Grasham et al., 2019; Saadabadi et al., 2019). Since SOFCs use gaseous fuels, TAN must be recovered as NH_3 gas, which can be achieved by vacuum (membrane) stripping. In SOFC, NH_3 is converted (together with oxygen)to nitrogen gas and water vapour, while no oxidised nitrogen species are formed (Okanishi et al., 2017; Staniforth and Ormerod, 2003). Therefore, SOFCs allow for the clean conversion of NH_3 while simultaneously energy is generated. However, because stripping NH_3 under vacuum also results in the evaporation of water (El-Bourawi et al., 2007; He et al., 2018), the gaseous permeate consists of a mixture of NH_3 gas and water vapour. Interestingly, Cinti et al. (2016) showed that it is actually possible to directly use gaseous NH_3-water mixtures as fuel for SOFC and that for higher concentrations of NH_3 in the fuel, the SOFC power density increases. Furthermore, El-Bourawi et al. (2007) showed that when the NH_3 concentration in the feed water of vacuum membrane stripping is increased, higher NH_3 fluxes and higher NH_3 concentrations in the gaseous permeate (NH_3-water mixture) are obtained. When higher NH_3 fluxes and higher NH_3 concentrations in the gaseous NH_3-water mixture can be obtained, the dimensions of the vacuum (membrane) stripping and SOFC units can be minimised. Therefore, high concentrations of NH_3 will lead to more efficient recovery and use of gaseous NH_3 for fertiliser production and energy generation purposes. By concentrating residual waters, high TAN concentrations can be obtained, as shown in previous studies in which TAN was concentrated as NH_4^+ by ED (Mondor et al., 2008; van Linden et al., 2019; Ward et al., 2018). However, because the pH of the concentrated streams were not actively increased, chemicals must be added to obtain concentrated dissolved NH_3.

1.4. Chemical addition to convert NH_4^+ to dissolved NH_3

The amount of added chemicals to increase the solution pH at standard temperature and pressure conditions (T = 25 °C and p = 101,325 Pa) to a certain value depends on the buffer capacity and the ionic strength of the solution. Various residual waters with high TAN concentrations, such as urine, reject water and industrial condensates contain buffering anions, such as bicarbonate (HCO_3^-). Fig. 1A depicts the effect of the buffer capacity on the required addition of sodium hydroxide (NaOH) to increase the solution pH from 7.8 to 10 for solutions with various TAN concentrations. Because HCO_3^- reacts with hydroxide (OH^-) to form carbonate (CO_3^{2-}), less OH^- is available to effectively increase the pH. Therefore, almost double the amount of NaOH is required to increase the pH in buffered solutions (NH_4HCO_3), compared to non-buffered solutions (NH_4Cl).

Besides, the ammoniacal nitrogen equilibrium pH (pK_a) increases when the ionic strength of the solution increases. Fig. 1B shows the distribution of NH_4^+ and NH_3 at standard conditions as a function of the pH for solutions with various TAN (as NH_4HCO_3) concentrations. The pK_a for a solution with a TAN concentration of 1.5 g L^{-1} is 9.4, while for 10 g L^{-1} the pK_a is 9.6, meaning that the pH must be further increased for solutions with TAN concentrations of 1.5 g L^{-1} to have the same amount of NH_4^+ and NH_3, compared to solutions with TAN concentrations of 10 g L^{-1}.

1.5. Bipolar membrane electrodialysis for NH_4^+ removal from waters

To avoid the addition of chemicals, bipolar membrane electrodialysis (BPMED) can be used to change the solution pH in situ by only using electrical energy (Mani, 1991; Tongwen, 2002). BPMED can be used to remove ions from a feed stream (the diluate) and simultaneously concentrate cations in a base stream (the base) and anions in an acid stream (the acid). The cations are combined with hydroxide ions (OH^-) in the base, while the anions are combined with protons (H^+) in the acid, which are produced in the bipolar membranes by dissociating water when an electric current is applied.

Previous studies showed that BPMED can be applied for the treatment of residual waters containing TAN mainly as NH_4^+. Various studies assessed the application of BPMED to produce dissolved NH_3 and acids such as HCl and HNO_3 from industrial residual waters containing NH_4Cl and NH_4NO_3, respectively (Ali et al., 2004; Graillon et al., 1996; Li et al., 2016; Lv et al., 2018). In addition, Pronk et al. (2006) and Shi et al. (2018) used BPMED for the recovery of nitrogen and phosphorus from source-separated urine and pig manure hydrolysate, respectively. Finally, Shuangchen et al. (2015) applied BPMED to recover CO_2 from spent NH_3-based carbon capture solutions.

1.6. Problem description

In previous studies, the efficiency of BPMED to use supplied electric charge (current efficiency) to produce acid and base was mainly limited by leakage of H^+, while also diffusion of NH_3 and leakage of OH^- through the membranes comprised the current efficiency (Ali et al., 2004; Graillon et al., 1996). However, these studies were conducted with high concentrations of NH_4^+ in the diluate (ranging 2–4 mol L^{-1} NH_4^+), at high current densities (ranging 480–900 A m^{-2}) and in absence of buffering anions such as HCO_3^- (Ali et al., 2004; Li et al., 2016; Lv et al., 2018). These feed water compositions and operational conditions are not representative for the application of BPMED on residual waters such as (sludge) reject water and industrial condensates, which have a typical NH_4^+ concentration ranging from 0.5 to 2.5 g L^{-1} (Gonzalez-Martinez et al., 2018). Besides, the previously conducted studies merely focused on the current efficiency of acid and base production, rather than on the current efficiency to transport NH_4^+ from the diluate (Ali et al., 2004; Li et al., 2016; Shuangchen et al., 2015). Finally, to our best knowledge, there are no studies available that assess the actual energy consumption to remove NH_4^+ from water by BPMED.

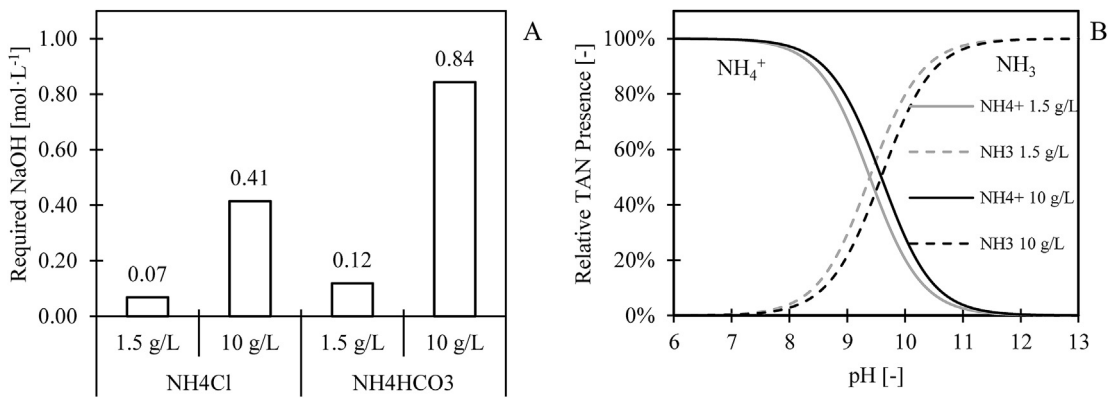

Fig. 1. The required NaOH addition to increase the pH from 7.8 to 10 for solutions containing NH_4Cl and NH_4HCO_3 (A). The ammoniacal nitrogen equilibrium pH shifts for TAN concentrations of 1.5 and 10 g L^{-1} (as NH_4HCO_3) from 9.4 to 9.6, respectively, as a result of an increase in ionic strength (B). Both graphs are derived from PHREEQC software simulations using the phreeqc.dat database.

1.7. Research objective

Therefore, in this study, we assessed the current efficiency and energy consumption to remove NH_4^+ from water by BPMED, while simultaneously producing concentrated dissolved NH_3. We focused on the processes affecting the current efficiency to transport NH_4^+ from the diluate. Furthermore, we compared the energy consumption of BPMED to the energy consumption of ED in combination with the addition of chemicals to remove NH_4^+ from water and produce concentrated dissolved NH_3.

2. Materials and methods

2.1. Materials

We used a bench-scale PC-Cell 64004 ED cell, consisting of a Pt/Ir-MMO coated and Ti-stretched metal anode and a stainless-steel cathode, both with a surface area of 8 × 8 cm^2. The cell contained a BPMED membrane stack consisting of ten cell triplets. Each cell triplet consisted of a cation exchange membrane (CEM), an anion exchange membrane (AEM) and a bipolar membrane (BPM), as depicted in Fig. 2. Two PCA SC cation exchange end membranes (CEEM) were placed next to the electrodes, similar to the studies conducted by Graillon et al. (1996) and Pronk et al. (2006) on BPMED and similar to our previous study on NH_4^+ removal by ED (van Linden et al., 2019). The rest of the BPMED membrane stack consisted of ten PCA Acid-60 AEMs, nine PCA SK CEMs and ten PCA BPMs. Specific membrane characteristics can be found through the supplier (PCA, 2016). The membranes and electrodes were separated by 0.5 mm thick wire mesh spacers with a void fraction of 59% made from silicon/polyethylene sulfone to form diluate, acid and base (flow) cells and electrode rinse compartments.

The electric current was applied by a Tenma 72–2535 power supply, having an electric current and electric potential range of 0.001–3.000 A and 0.01–30.00 V, respectively.

The diluate, acid, base and electrode rinse solutions were stored in 1 L borosilicate bottles and were continuously mixed by magnetic stirrers on a mixing plate. The solutions were recirculated through the BPMED membrane stack by a calibrated peristaltic Watson-Marlow 520S pump with separate Watson-Marlow 313 pump heads for each solution. The pump was set at a flow rate of 19 L h^{-1}, corresponding to a cross-flow velocity of 2 cm s^{-1} in the diluate, acid and base cells. The diluate, acid and base pH were measured in the respective bottles, using three calibrated IDS SenTix 940 pH sensors and a WTW Multi 3630 IDS multimeter. The acid and base EC were also measured in the respective bottles, using two calibrated TetraCon 925 EC-sensors and a separate multimeter. The diluate EC was measured in the respective bottle with a separate EC-sensor and multimeter. Fig. 3 presents a schematic representation of the complete experimental BPMED set-up.

TAN concentrations were measured with Machery-Nagel NANOCOLOR Ammonium 200 (range: 0.04–0.2 g L^{-1}) and 2,000 (range: 0.4–2.0 g L^{-1}) test kits. We used calibrated volumetric cylinders to determine the solution volumes.

The initial diluate, acid and base solutions contained 6.6 g NH_4HCO_3 in 1 L of demi water, corresponding to an NH_4^+ concentration of 1.5 g L^{-1}, which is a representative concentration of residual waters such as (sludge) reject water and certain industrial condensates. The initial electrode rinse solutions consisted of 1 M $NaNO_3$ (addition of $NaNO_3$ to 1 L of demi water). It must be noted that due to BPMED membrane stack configuration (equipped with CEEMs) and the use of $NaNO_3$ in the initial electrode rinse solution, NH_4^+ can be transported to the electrode rinse at the cathode, while sodium (Na^+) can be washed-out from the electrode rinse at the anode, as depicted in Fig. 2.

Finally, for the NH_3 diffusion experiment, Acros Organics 25% NH_4OH and NaCl were used. All used salts were of analytical grade (Sigma Aldrich Reagent Plus, ≥ 99%). All experiments were conducted at a temperature of 24 ± 2 °C (AVG ± STD, n = 20).

2.2. Methods

2.2.1. Removal of NH_4^+ and production of concentrated dissolved NH_3

To assess the current efficiency and energy consumption to remove NH_4^+ from water by BPMED, while simultaneously producing concentrated dissolved NH_3, we performed duplicate sequencing batch experiments (SBEs). For the first batch of the SBEs, new diluate, acid, base and electrode rinse solutions were used. The diluate EC of each consecutive batch was decreased to 1 mS cm^{-1} by applying dynamic current density, as described in our previous work (van Linden et al., 2019), where we showed that the decrease of the diluate EC to 1 mS cm^{-1} corresponds to 90% removal of NH_4^+ from the new diluate solutions. The removal of NH_4^+ by 90% is comparable to state-of-the-art NH_4^+ removal technologies such as anammox and air stripping. In both ED and BPMED, the diluate is determining for the limiting current density. Therefore, because the same diluate solution, spacer geometry and cross-flow velocity were used, the same procedure of dynamic current density application as in our previous study was followed,

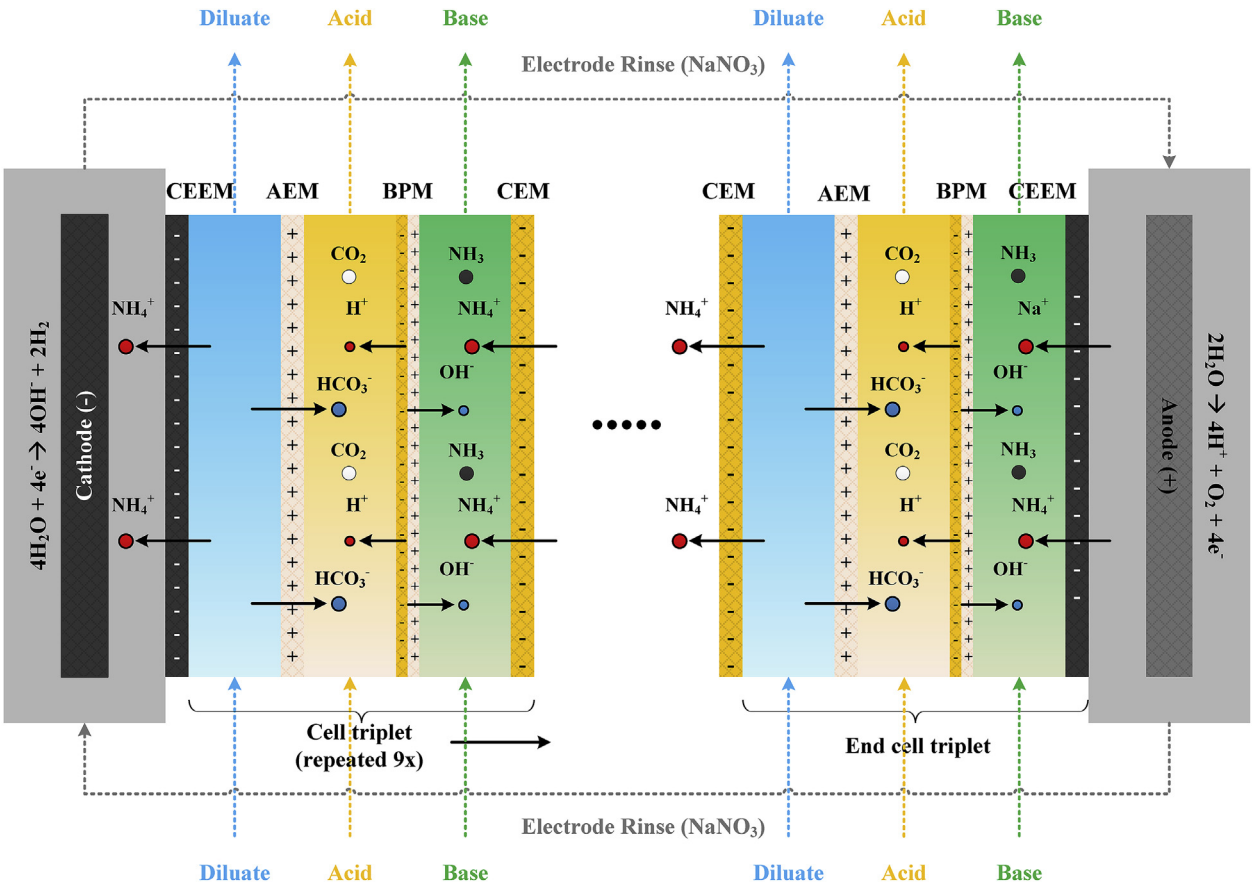

Fig. 2. The membrane and (flow) cell sequence in the BPMED membrane stack and the intended ion transport (electro-migration and water dissociation) as a result of the applied current. In the acid, H^+ and HCO_3^- are combined and react to CO_2, while in the base OH^- and NH_4^+ are combined and react to NH_3. At the cathode, NH_4^+ is transported to the electrode rinse, while at the anode, both Na^+ and NH_4^+ are transported to the base, resulting in the accumulation of NH_4^+ in the electrode rinse and the wash-out of Na^+ to the base.

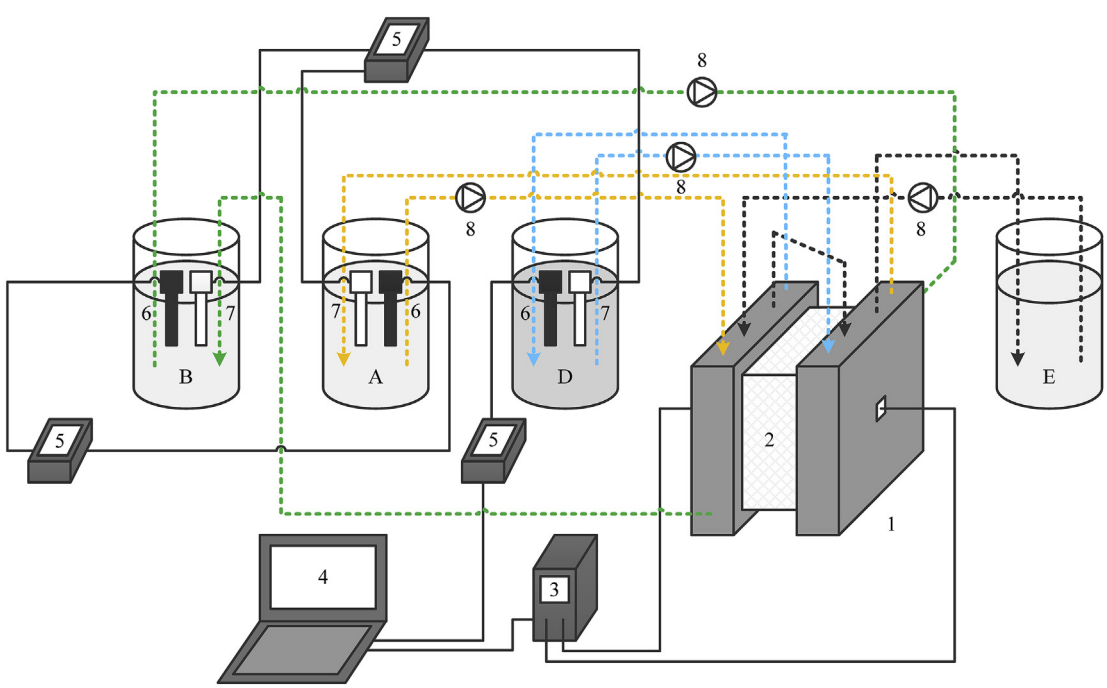

Fig. 3. The used experimental set-up, including the cell (1), the BPMED membrane stack (2), power supply (3), laptop (4), multimeters (5), EC-sensors (6), pH-sensors (7), peristaltic pumps (8) and the diluate (D), acid (A), base (B) and electrode rinse (E) bottles and solutions.

using a safety factor of 0.62 (van Linden et al., 2019). When the diluate EC was decreased from 8 to 1 mS cm^{-1}, the treated diluate batch was replaced by a new diluate batch, while the acid, base and electrode rinse batches were recycled. Solution volumes and TAN concentrations were measured at the beginning and end of each batch to assess the water and TAN mass balance. In addition, the electric current and electric potential were automatically logged every 5 seconds on a laptop. Finally, the EC and pH of the diluate, acid and base were also logged automatically every 5 seconds, while the EC and pH of the electrode rinse were manually measured at the beginning and end of each batch.

2.2.2. Diffusion of NH_3 through the BPMED membrane stack

Additionally, we performed a diffusion experiment to study the diffusion of NH_3 through the BPMED stack. During this experiment, a 1 L base solution containing NH_3 (NH_4OH in demi water) was recirculated through the same BPMED membrane stack as used in the SBEs. In addition, 1 L diluate and acid solutions without NH_3 (demi water) were also recirculated through the BPMED stack. NaCl was added to the diluate, acid and base, to obtain equal ionic strengths (corresponding to an EC of 8 mS cm^{-1}) to minimise osmotic water transport. A 1 L solution consisting of 1 M $NaNO_3$ was again used as electrode rinse. The same hydraulic conditions were used for the diffusion experiment as during the SBEs, but no electric current was applied. TAN concentrations were measured in all solutions every hour and the diluate, acid, base and electrode rinse pH and EC were measured and logged automatically every 5 min. Finally, initial and final solution volumes were again determined to assess the water and TAN mass balance.

2.2.3. Avoiding accumulation of TAN in the electrode rinse

Finally, we aimed to limit the accumulation of TAN in the electrode rinse. To this end, we constructed a BPMED membrane stack equipped with AEEMs, by replacing the CEEMs of the original BPMED membrane stack by additional identical AEMs used in the original BPMED membrane stack. The membrane sequence was adjusted in such a way that again ten cell triplets were formed. A schematisation with the membrane configuration of the BPMED membrane stacks equipped with CEEMs and AEEMs can be found in the Supporting Information (Fig. SI.1). We repeated only the first batch of the SBEs with the adjusted BPMED membrane stack (in duplicate), at identical operational conditions and applied settings and used the same analytical procedures.

2.3. Performance indicators

As a measure for the utilisation of electric charge to transport NH_4^+ from the diluate, we assessed the NH_4^+ current efficiency. The NH_4^+ current efficiency represents the efficiency to transport NH_4^+ by electro-migration from the diluate through the CEMs. Ideally, the charge transported as NH_4^+ is equal to the supplied electric charge, but diffusion and leakage processes and the transport of other cations through the CEM all decrease the NH_4^+ current efficiency. The NH_4^+ current efficiency was determined by the ratio between the charge equivalent transported as NH_4^+ and the supplied electric charge (Eq. (1)).

$$\eta_{NH_4^+} = \frac{z \cdot F \cdot n_{NH_4^+,d}}{N \cdot \sum_{t=0}^{t} \left(I_{\Delta t} \cdot \Delta t \right)} \cdot 100\% \tag{1}$$

Where η_{NH4+} = NH_4^+ current efficiency (unitless), z = ion valence (unitless, z = 1 for NH_4^+), F = Faraday constant (in $C \cdot mol^{-1}$, F = 96,485 C mol^{-1}), $n_{NH4+,d}$ = amount of NH_4^+ transported from the diluate (in mol), N = number of cell triplets in the BPMED membrane stack (unitless, N = 10), $I_{\Delta t}$ = average electric current during each time interval (in A = $C \cdot s^{-1}$) and Δt = time interval (in s).

Furthermore, we determined the electrochemical energy consumption to transport NH_4^+ from the diluate by BPMED, based on the consumed electrical energy and the transported NH_4^+ mass (Eq. (2)).

$$E_e = \frac{\sum_{t=0}^{t} \left(U_{\Delta t} \cdot I_{\Delta t} \cdot \Delta t \right)}{m_{NH_4^+,d}} \tag{2}$$

Where E_e = electrochemical energy consumption (in $J \cdot g\text{-}N^{-1}$), $U_{\Delta t}$ = average electric potential during each time interval (in V) and $m_{NH4+,d}$ = amount of transported NH_4^+ from the diluate (in g-N).

3. Results

3.1. Removal of NH_4^+ and production of concentrated dissolved NH_3

The reported values represent the average results of the duplicate SBEs, unless indicated differently. The deviation (minimum and maximum) of the duplicate results was always below 10%. Fig. 4A presents the diluate, acid and base EC over the cumulative electrochemical energy consumption throughout one SBE. In the Supporting Information, the evolution of the EC and pH throughout the duplicate SBE is presented (Fig. SI.2). The diluate EC for each new batch was decreased from 8 to 1 mS cm^{-1}. For each consecutive diluate batch, more time was needed to decrease the diluate EC to 1 mS cm^{-1}. The operational run time increased from 66 min for the first batch to 89 min for the tenth batch. However, the increase in operational run time did not result in an increase in electrochemical energy consumption per batch, as for the first batch 18.7 kJ was used and for the tenth batch 18.1 kJ was used. The base EC increased steadily throughout the SBEs and finally reached 18 mS cm^{-1}. The acid EC only increased from 8 to 10 mS cm^{-1} during the first three batches. Subsequently, the increase in acid EC accelerated and the acid EC exceeded the base EC after six batches. The acid EC reached a final value of 25 mS cm^{-1}.

Fig. 4B presents the pH of the diluate, acid and base. The base pH increased during the first five batches and subsequently reached a plateau at 9.8. The acid pH decreased from 7.8 to 6.5 after the first two batches and subsequently increased for each consecutive batch, eventually reaching 7.3 after the tenth batch. The new diluate batches had an average pH of 7.8 and for each batch after the first batch, the diluate pH increased and reached 9.1 after the tenth batch.

According to Fig. 5A, the decrease in diluate EC to 1 mS cm^{-1} corresponded to a TAN removal efficiency ranging 85–91%. The amount of transported NH_4^+ was 1.3 ± 0.1 g (AVG ± STD, n = 20) for consecutive batches in duplicate. For the first five batches, at least 90% of TAN was removed from the diluate, but the TAN removal efficiency decreased to 85% for the tenth batch. The TAN concentration in the base increased from 1.5 to 7.3 g L^{-1}, corresponding to a concentration factor of 5. Based on the intended ion transport (Fig. 2), no NH_4^+ transport should take place to the acid. However, the TAN concentration in the acid increased from 1.5 to 5.4 g L^{-1} and showed a first-order kinetics trend (accelerating increase). Finally, the TAN concentration also increased in the electrode rinse, from 0 to 3.4 g L^{-1}. In the Supporting Information, the evolution of the TAN and NH_3 concentrations throughout the duplicate SBE is presented (Fig. SI.3). The water and TAN mass balance of all batches fitted with an average error of 3%.

Fig. 5B presents the actual NH_3 concentrations throughout the

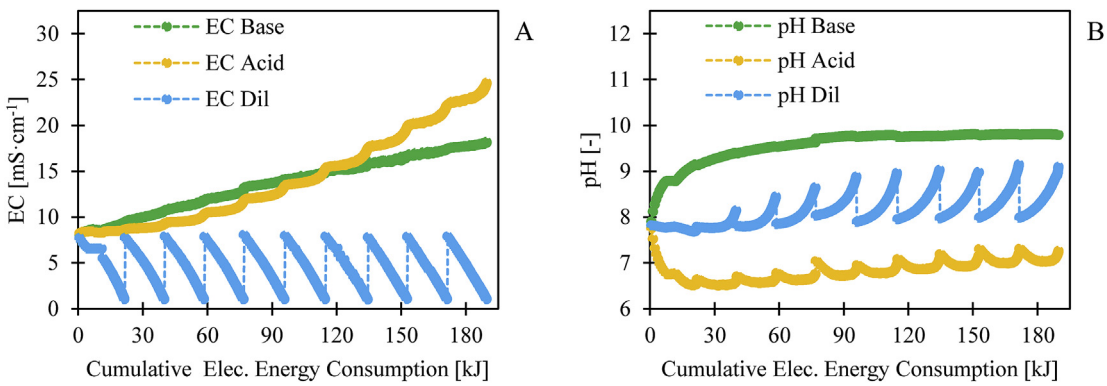

Fig. 4. The EC (A) and pH (B) throughout one of the SBE duplicates. The diluate EC decreased to 1 mS cm^{-1} for each batch, while the acid and base EC increased to 25 and 19 mS cm^{-1} throughout the SBE, respectively. The diluate pH increased during each batch and the final diluate pH increased over the consecutive batches from 7.8 to 9.1. The base pH increased throughout the SBEs and reached a plateau at 9.8, while the acid pH initially decreased to 6.5 and subsequently increased each consecutive batch to a final value of 7.3.

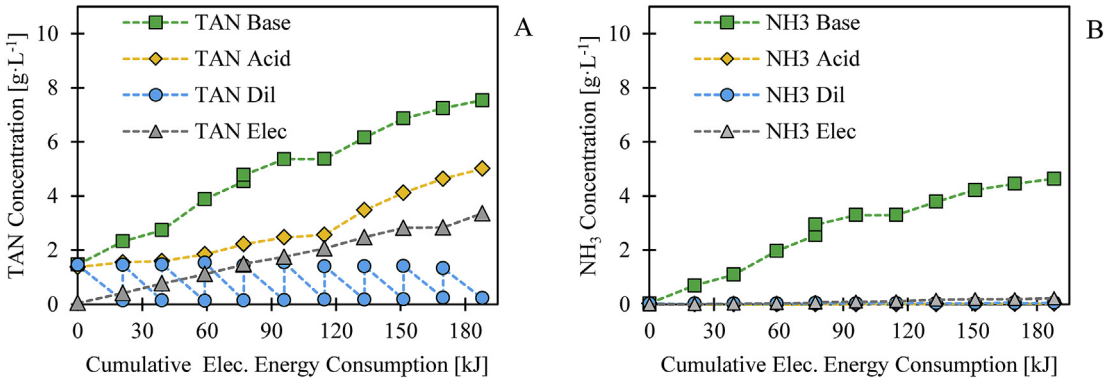

Fig. 5. The concentrations of TAN (A) and NH_3 (B) in the diluate, acid, base and electrode rinse throughout one of the SBE duplicates. The removal efficiency of TAN from the diluate decreased from 91% for the first batch to 85% for the tenth batch. The transported NH_4^+ partially ended to the base, which had a final pH of 9.8, resulting in a final NH_3 concentration in the base of 4.5 g L^{-1}. The residual fraction of the transported NH_4^+ ended up as NH_4^+ in the acid and the electrode rinse.

SBEs, as calculated based on the measured TAN concentrations, temperature, pH and ionic strength in the various solutions. The concentration of NH_3 in the base increased from 0 to 4.5 g L^{-1} after the tenth batch. On the other hand, the NH_3 concentration in the diluate, acid and electrode rinse throughout the SBE never exceeded 0.2 g L^{-1}. Due to the accumulation of NH_3 in the base, an NH_3 concentration gradient, ranging 0.7–4.5 g L^{-1}, established between the base and diluate and the base and acid.

Fig. 6A shows that the NH_4^+ current efficiency decreased from 69% for the first batch to 54% for the tenth batch throughout the SBEs. Interestingly, according to Fig. 6B, the electrochemical energy consumption to remove NH_4^+ by 85–91% was stable at 18 ± 1 MJ·kg-N^{-1} (AVG ± STD, n = 20).

3.2. Diffusion of NH_3 through the BPMED membrane stack

Fig. 7 presents the NH_3 concentrations throughout the additionally conducted diffusion experiment, during which no electric current was applied. The NH_3 concentrations are again calculated based on the measured TAN concentrations, temperature, pH and ionic strength of the solutions. The pH of the diluate, acid and base pH was always higher than 10.3 after the start of the experiment, indicating that TAN was present as NH_3 for at least 90%. The initial NH_3 concentration in the base was 12.5 g L^{-1} and decreased to 6.4 g L^{-1} after 480 min, showing a decelerating trend. The NH_3 concentration in the diluate and acid increased, also showing a decelerating trend. The concentration of NH_3 in the diluate and the acid increased from 0 to 2.4 and 3.1 g L^{-1}, respectively. The NH_3 concentration in the electrode rinse throughout the diffusion experiment did not exceed 0.02 g L^{-1}. The NH_3 mass balance of the diffusion experiment fitted with an error of 6%. The error was probably caused by volatilisation of NH_3 at these high NH_3 concentrations and long operational run time.

Due to the decrease in NH_3 concentration in the base and increase in NH_3 in the diluate and acid, the NH_3 concentration gradient between the base and acid and the base and diluate decreased over time, from 12.5 g L^{-1} to 3.3 g L^{-1} and 4.0 g L^{-1}, respectively. The NH_3 concentration gradient between the diluate and acid increased from 0 to only 0.8 g L^{-1}.

3.3. Avoiding accumulation of TAN in the electrode rinse

During the duplicate SBEs, 27 ± 11% (AVG ± STD, n = 20) of the TAN transported from new diluate batches ended up and accumulated as NH_4^+ in the electrode rinse, resulting in a final TAN concentration in the electrode rinse of 3.4 g L^{-1}. The observed accumulation of TAN in the electrode rinse was similar to the findings in our previous study (van Linden et al., 2019), in which we used ED to remove TAN as NH_4^+ from the same diluate. Fig. 8 shows that during the first batch of the duplicate SBEs 26% of the TAN transported from the diluate accumulated in the electrode rinse when the BPMED membrane stack was equipped with CEEMs. Concurrently, only 64% of the TAN transported from the diluate accumulated in the base.

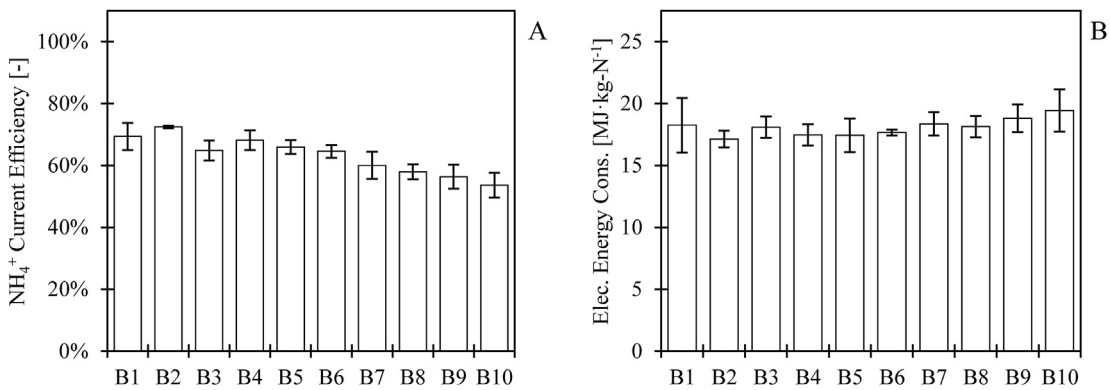

Fig. 6. The NH_4^+ current efficiency (A) decreased over the consecutive batches from 69% to 54%, while the electrochemical energy consumption (B) to remove NH_4^+ by 85–91% remained stable at 18 MJ·kg-N^{-1} over the consecutive batches. Average values of the duplicate SBEs are presented, along with the minimum and maximum values (outer values of error bars).

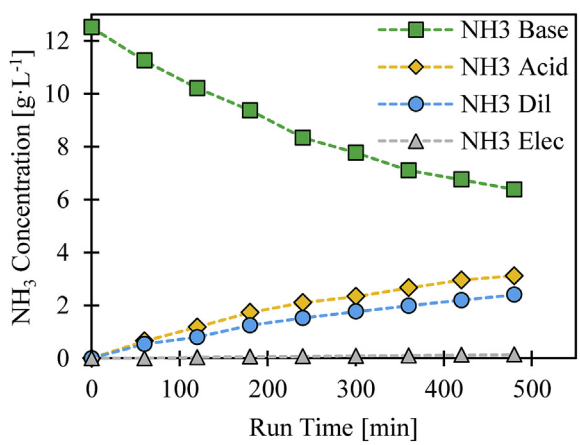

Fig. 7. The NH_3 concentration in the base decreased during the diffusion experiment due to NH_3 diffusion from the base to the diluate and the acid.

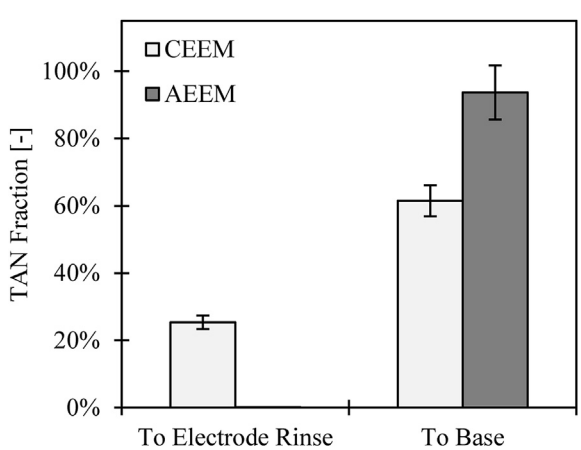

Fig. 8. The accumulation of TAN transported from the diluate in the electrode rinse decreased from 26% for the use of CEEMs to 0% for the use of AEEMs in the BPMED membrane stack. In addition, the accumulation of TAN transported from the diluate in the base increased from 64% for the use of CEEMs to 94% for the use of AEEMs. Average values of the duplicate experiments are shown, along with the minimum and maximum values (outer values of the error bars).

During the experiments with a BPMED membrane stack with AEEMs, the fraction of TAN that accumulated in the electrode rinse was negligible, while the fraction of TAN that accumulated in the base increased to 94%.

4. Discussion

4.1. Removal of NH_4^+ and production of concentrated dissolved NH_3

4.1.1. Evaluation of the diluate

The decrease in diluate EC from 8 to 1 mS cm^{-1} (Fig. 4A) was the result of the effective removal of NH_4^+ and HCO_3^- from the diluate. The diluate pH increased during the treatment of new diluate batches (Fig. 4B), in contrast to multiple previous studies (Li et al., 2016; Shi et al., 2018). Two phenomena probably caused the increase in diluate pH. Firstly, diffusion of NH_3 from the base, which was validated to take place in the diffusion experiment (3.3), resulted in the consumption of H^+ in the diluate to form NH_4^+, leading to the diluate pH increase. Secondly, the diluate pH increased due to leakage of OH^- from the base to the diluate. OH^- is prone to leak through CEMs due to, amongst others, its high diffusivity (H. Strathmann, 2010). The effect of NH_3 diffusion and OH^- leakage on the diluate pH became more apparent at the end of each batch (Fig. 4B), when the concentration gradients were highest and the buffer capacity of the diluate was decreased, due to the removal of NH_4^+ and HCO_3^-. Apparently, NH_3 diffusion and OH^- leakage affected the diluate pH more than any diffusion of CO_2 or leakage of H^+ from the acid, which would cause a decrease in the diluate pH. Because the operational run time and the NH_3 and OH^- concentration gradients between the base and diluate increased throughout the SBEs, the final diluate pH increased from 7.7 for the first batch to 9.1 for the tenth batch. The decrease in NH_4^+ removal efficiency from 91 to 85% over the consecutive batches was also a result of the diluate pH increase throughout each batch. Due to the pH increase, a fraction of the NH_4^+ was converted to NH_3 and was therefore not transported by electro-migration.

4.1.2. Evaluation of the base

The base pH reached a plateau at pH = 9.8 (Fig. 4B), whereas in previous studies pH values higher than 11 were achieved (Li et al., 2016; Shi et al., 2018). One of the causes of the plateauing of the base pH was the consumption of OH^- by NH_4^+, resulting in the formation of NH_3 (and water). Therefore, a certain fraction of OH^- produced by the BPMs was not translated to an increase in base pH. Besides, in contrast to previous studies, the initial base contained HCO_3^-, which reacted with the produced OH^- to CO_3^{2-}. Finally, any diffusion of CO_2 from the acid also contributed to the plateauing of the base pH, as CO_2 reacts with OH^- to HCO_3^-. Therefore, not all produced OH^- was available to increase the pH effectively. The OH^- concentration gradient between the base and diluate increased from $1.2 \cdot 10^{-5}$ to $4.9 \cdot 10^{-5}$ mol L^{-1} throughout the SBEs. At a final

base pH of 9.8, a temperature of 24 °C and an EC of 18 mS cm^{-1}, 71% of the TAN was present as NH_3. The NH_3 concentration in the base increased from 0 to 4.5 g L^{-1}, while the NH_4^+ concentration in the base increased from 1.5 to 2.9 g L^{-1}. Eventually, only 48 ± 21% (AVG ± STD, n = 20) of the NH_4^+ transported from the diluate accumulated in the base. The residual NH_4^+ transported from the diluate accumulated in the acid and the electrode rinse. As mentioned in 2.1, the transport of NH_4^+ to the electrode rinse led to the wash-out of Na^+ from the electrode rinse, resulting in the accumulation of Na^+-species (such as NaOH, $NaHCO_3$ and Na_2CO_3) in the base. NH_4^+ and Na^+ accumulated with the anions OH^-, HCO_3^- and CO_3^{2-} in the base, explaining the increase in base EC (Fig. 4A). Of these anions, OH^- was produced by the BPMs, while HCO_3^- either diffused as CO_2 (as mentioned by Pronk et al. (2006)) or as HCO_3^--species from the acid and CO_3^{2-} was formed by OH^- and HCO_3^-. The NH_3 and NH_4^+ concentration gradients between the base and diluate ranged 0.04–0.27 mol L^{-1} and 0.08–0.15 mol L^{-1}, respectively.

4.1.3. Evaluation of the acid

The limited increase in acid EC after the first three batches (Fig. 4A) was a result of the formation of uncharged CO_2 from the produced H^+ and the transported HCO_3^- in the acid. Because CO_2 has a relatively low solubility (1.5 g L^{-1} at T = 24 °C, based on the Henry's constant and thermodynamic data taken from Sander (2015)), it became supersaturated in the acid, indicated by the observation of obvious gas bubbles. The transport of gas bubbles to the headspace of the acid solution bottle indicated spontaneous stripping of CO_2 from the acid. In previous studies, H^+ accumulated in the acid with ions such as Cl^-, resulting in H^+ leakage from the acid to the diluate and ultimately a decrease in diluate pH (Li et al., 2016; Shi et al., 2018). Because in this study HCO_3^- was the main anion, accumulation of H^+ in the acid and leakage of H^+ to the diluate was limited because a part of H^+ reacted with HCO_3^- to form CO_2 (and water). Interestingly, after the sixth batch, the increase in acid EC and also TAN concentration accelerated (Figs. 4A and 5A). Because the operational run time and the NH_3 concentration gradient between the base and acid both increased throughout the SBEs, more NH_3 diffusion to the acid took place. The diffused NH_3 reacted in the acid with H^+, causing the accelerated increase in acid EC and TAN concentration. Besides, the acid pH increased each consecutive batch after the first two batches (Fig. 4B), due to NH_3 diffusion and OH^- leakage from the base.

4.1.4. Assessment of the NH_4^+ current efficiency

For the treatment of each consecutive diluate batch, a loss in NH_4^+ current efficiency was observed (Fig. 6B). The loss in NH_4^+ current efficiency was caused by the leakage of OH^-, the diffusion of dissolved NH_3 and diffusion of ionic species (such as Na^+-species and TAN-species). Because a concentration gradient was present, TAN-species such as NH_4HCO_3 could diffuse from the base back to the diluate. Therefore, to decrease the diluate EC to 1 mS cm^{-1}, NH_4^+ was transported back and forth, at the expense of additional electric charge. Besides, the accumulated Na^+-species could also diffuse from the base to the diluate and therefore contribute to the loss in NH_4^+ current efficiency. The mentioned OH^- leakage, dissolved NH_3 diffusion and diffusion of TAN-species and Na^+-species (the ionic species) all took place from the base, through the CEMs, to the diluate. The contribution of H^+ leakage in the form of proton or hydronium (H_3O^+) ions was neglected, because the H^+ concentration gradient was at least two orders of magnitude lower than the NH_3, OH^- and ionic species concentration gradients between the base and the diluate. Also electro-migration of H^+ was neglected because the amount of charge in the new diluate batches represented by H^+ was only $1 \cdot 10^{-3}$ C, compared to approximately 8,000 C for NH_4^+ (corresponding to 1.5 g NH_4^+).

Because a fixed amount of TAN mass was transported per batch of new diluate, a fixed amount of charge as NH_4^+ was transported. Therefore, according to Eq. (1), the loss in NH_4^+ current efficiency was a result of additionally supplied electric charge. Because the leakage and diffusion processes partially counteracted the intended decrease in diluate EC, the operational run time to treat the new diluate batches increased and more electric charge was supplied. As a result, the NH_4^+ current efficiency decreased over consecutive batches, as depicted in Fig. 6A. Ultimately, the decrease in NH_4^+ current efficiency throughout the SBEs was a result of both the increase in operational run time and concentration gradients, which led to more OH^- leakage and dissolved NH_3 and ionic species diffusion. However, based on the available data, no conclusions can be drawn on what process (OH^- leakage, dissolved NH_3 or ionic species diffusion) had the largest contribution to the loss in NH_4^+ current efficiency.

4.1.5. Assessment of the electrochemical energy consumption

Even though the NH_4^+ current efficiency decreased over the consecutive batches, the electrochemical energy consumption to remove NH_4^+ by 85–91% was stable at 18 MJ·kg-N^{-1} (Fig. 6B). The decrease in NH_4^+ current efficiency was compensated by a decrease in electric potential throughout the SBEs. Fig. 9 shows that the average electric potential throughout a batch decreased over the consecutive batches. The average electric potential was 15.5 V for the first batch and dropped to 12.6 V for the tenth batch. The decrease in electric potential was a result of the increase in acid and base EC throughout the SBEs (Fig. 4A), which led to a decrease of the electrical resistance of the BPMED membrane stack.

4.2. Diffusion of NH_3 through the BPMED membrane stack

During the diffusion experiment (Fig. 7), diffusion of NH_3 took probably place from the base (through the BPMs) to the acid and (through the CEMs) to the diluate, as the NH_3 concentration gradients between the base and acid and the base and diluate (ranging 3.3–12.5 g L^{-1}) were at least four times higher than the NH_3 concentration gradient that between the diluate and acid (ranging 0.0–0.8 g L^{-1}). Furthermore, the decelerated changes (first-order kinetics) in NH_3 concentrations in the base, acid and diluate during the diffusion experiment were caused by the decrease in NH_3

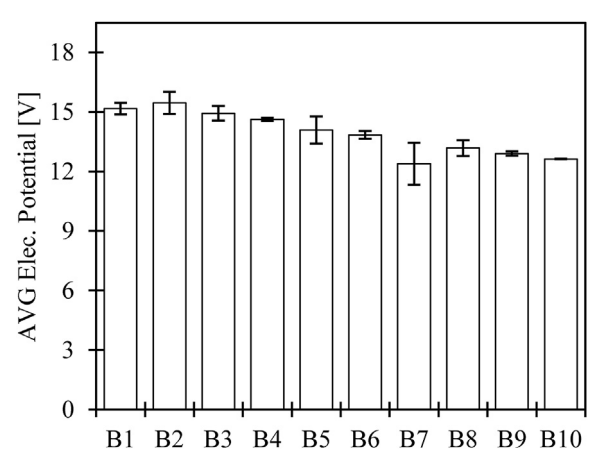

Fig. 9. The average electric potentials during each consecutive batch decreased throughout the SBEs due to a decrease in electrical resistance of the BPMED membrane stack as a result of the increase in acid and base EC. Average values of the duplicate experiments are shown, along with the minimum and maximum values (outer values error bars).

concentration gradients, which is typical for diffusion experiments. The NH_3 concentration in the acid was always higher than in the diluate, suggesting that NH_3 diffused more easily from the base, through the BPMs, to the acid than from the base, through the CEMs, to the diluate. Even though diffusion of NH_3 through CEMs and BPMs is reported previously (Ali et al., 2004), drawing firm conclusions on what membranes are more susceptible to NH_3 diffusion requires the determination of membrane permeability constants.

4.3. Avoiding accumulation of TAN in the electrode rinse

According to the results of the diffusion experiment in 3.3, the transport of TAN to the electrode rinse by diffusion of NH_3 from the base was negligible. Therefore, the main mechanism responsible for the transport of TAN to the electrode rinse was electro-migration of NH_4^+, while TAN-species could also diffuse from and to the electrode rinse. During the SBEs, TAN was transported as NH_4^+ by electro-migration from the diluate, through the CEEM at the cathode, to the electrode rinse. Because the electrode rinse consisted of $NaNO_3$, both Na^+ and NH_4^+ were transported from the electrode rinse, through the CEEM at the anode, to the base (Fig. 2), resulting in the accumulation of NH_4^+ in the electrode rinse and the wash-out of Na^+.

By replacing CEEMs by AEEMs in the BPMED membrane stack, electro-migration to the electrode rinse was prevented and the transport of TAN to the base increased (Fig. 8), suggesting that higher TAN and NH_3 concentrations potentially can be achieved in the base when the same amount of diluate is treated. Furthermore, the use of AEEMs in the BPMED membrane stack also resulted in an increase in NH_4^+ current efficiency from 69 to 78% and a decrease in electrochemical energy consumption from 18 to 16 MJ·kg-N^{-1}. The observed increase in NH_4^+ current efficiency and decrease in energy consumption may be explained by the avoided diffusion of Na^+-species from the base to the diluate, as wash-out of Na^+ was avoided.

The results show that the use of AEEMs instead of CEEMs in the BPMED membrane stack effectively prevented the accumulation of TAN in the electrode rinse, without notable negative side-effects. However, in this membrane stack configuration and the use of $NaNO_3$ as initial electrode rinse solution, HCO_3^- can accumulated in the electrode rinse, at the expense of the anion initially present in the electrode rinse (NO_3^-). To avoid the wash-out of NO_3^- from the electrode rinse, it could be considered to use HCO_3^- as an anion in the initial electrode rinse, to further limit accumulation and wash-out of ions. Another option is to equip the BPMED membrane stack with CEEMs and use NH_4^+ as cation for the initial electrode rinse. The latter would not require an adjustment in the initially used BPMED membrane stack configuration containing CEEMs.

4.4. Energetic evaluation of BPMED and ED in combination with the addition of chemicals

The electrochemical energy consumption to transport NH_4^+ by BPMED was three times as much compared to the 5.4 MJ·kg-N^{-1} reported for ED in our previous study (van Linden et al., 2019). The difference in electrochemical energy consumption is partially explained by the lower NH_4^+ current efficiency of BPMED, compared to ED. The NH_4^+ current efficiency of BPMED ranged 54–69%, whereas the NH_4^+ current efficiency of ED ranged 83–96%. Thus, for BPMED more electric charge was required to transport the same amount of NH_4^+. In addition, the average electric potential during a batch for BPMED (ranging 12.6–15.2 V) was higher than for ED (ranging 5.7–7.0 V). The higher electric potential for BPMED was a result of the presence of additional cells and the presence of BPMs. While ED membrane stacks contain cell pairs (diluate and concentrate), BPMED membrane stacks contain cell triplets (diluate, acid and base). The addition of extra cells introduces additional electrical resistance of the membranes, liquids and the spacers. Besides, BPMED makes use of BPMs, which introduce an electrical resistance and an additional electric potential for the dissociation of water, depending on the pH gradient between the acid and base (Mani, 1991). For BPMED, 30% more electric charge was required than for ED, whereas the electric potential for BPMED was 130% higher than for ED. Together, the extra electric charge and the higher electric potential explain the higher electrochemical energy consumption of BPMED to transport NH_4^+.

Besides the energy to drive the electrochemical processes, energy is required to pump the solutions through the ED cell. We determined the pumping energy based on additional hydraulic pressure measurements over the membrane stack and the respective hydraulic flow rates. The hydraulic pressure loss at a flow rate of 19 L h^{-1} was 9.3 kPa for the diluate, acid and base, having ten cells each. In addition, the hydraulic pressure loss for the electrode rinse was 8.4 kPa. With a maximum operational run time of 89 min for BPMED and 66 min for ED, the pumping energy was 1.0 kJ and 0.5 kJ, respectively. More information on the determination of the pumping energy is presented in the Supporting Information.

In our previous study, we produced a concentrate solution with a TAN concentration of 10 g L^{-1}, which was present as NH_4HCO_3 (van Linden et al., 2019). To compare the energy consumption of BPMED and ED for the removal of NH_4^+ and simultaneous production of NH_3, an equal NH_3 concentration should be taken as a reference point. In this study, after ten batches, we produced a base solution with a TAN concentration of 7.3 g L^{-1} at a pH of 9.8, corresponding to an NH_3 concentration of 4.5 g L^{-1}. To achieve this, in total 13 g of TAN was transported as NH_4^+ from the diluate by BPMED. For ED, seven identical diluate batches (1 L solutions containing 1.5 g L^{-1} TAN as NH_4HCO_3) were treated the same way (decrease of EC to 1 mS cm^{-1}) to produce a concentrate solution with a TAN concentration of 7.3 g L^{-1}, corresponding to the transport of 10 g of TAN as NH_4^+ from the diluate. However, the final pH of the ED concentrate only reached 8.8. Therefore, we determined with PHREEQC software how much NaOH must be added to increase the pH to 9.8 and calculated how much energy is associated with the industrial production of NaOH. According to the study of Hong et al. (2014) on the life cycle analysis of NaOH production, 2,176 kWh of electricity is consumed to produce one ton of NaOH by electrolysis, which corresponds to 7.8 kJ·g-NaOH^{-1}.

Table 1 presents the amount of required NaOH to increase the pH from 8.8 to 9.8 of the ED concentrate. When the energy consumption for driving the electrochemical processes, pumping and chemical production is considered, BPMED appears to be energetically competitive to ED in combination with the addition of chemicals. The energy consumption to produce 4.5 g L^{-1} NH_3 by BPMED and ED with the addition of chemicals was 19 and 22 MJ·kg-N^{-1}, respectively.

4.5. Future outlook

We showed that BPMED can be applied successfully to remove 85–91% NH_4^+ from water and simultaneously produce concentrated dissolved NH_3. We identified OH^- leakage, dissolved NH_3 diffusion and ionic species diffusion as main processes limiting the current efficiency to transport NH_4^+. By increasing the NH_4^+ current efficiency, the electrochemical energy consumption to remove NH_4^+ by BPMED can be decreased. To this end, the effect of OH^- leakage, dissolved NH_3 diffusion and ionic species diffusion must be minimised.

Table 1
The energetic evaluation of the production of a solution with an NH_3 concentration of 4.5 g L^{-1} by BPMED and ED, including on the energy input to drive the electrochemical processes, the pumping energy to recirculate the solutions and the energy to produce chemicals.

		Unit	BPMED Base	ED Concentrate
Solution Conditions	Final TAN	$g \cdot L^{-1}$	7.3	7.3
	Final pH	–	9.8	8.8
Chemical Addition	NaOH	g	–	16.5
Energy	Electrochem.	kJ	$18 \cdot 10 = 180$	$5.4 \cdot 7 = 38$
	Pumping	kJ	$1.0 \cdot 10 = 10$	$0.5 \cdot 7 = 3.5$
	NaOH	kJ	–	129
Mass Transported	NH_4^+	g	13	10
Total Energy Consumption		$MJ \cdot kg\text{-}N^{-1}$	19	22

Since concentration gradients cannot be avoided in BPMED due to the production of concentrated NH_3 in the base, the permeability of the CEMs for OH^- leakage, dissolved NH_3 diffusion and ionic species diffusion must be decreased. The OH^- permeability of CEMs may be decreased by adjusting the membrane materials and structure, as was successfully done for the H^+ permeability of AEMs (Gineste et al., 1996). Furthermore, Ali et al. (2004) used various CEMs in their study and mentioned that the NH_3 permeability of certain CEMs was lower than for others, indicating that the permeability of NH_3 depends on the type of CEM, suggesting that the use of other CEMs than we used in this study could limit the diffusion of NH_3.

Furthermore, the NH_4^+ current efficiency can be increased by decreasing the operational run time. The latter can be achieved by increasing the cross-flow velocity, allowing for a higher limiting current density (Heiner Strathmann, 2004). The current density can also be increased by increasing the applied safety factor for dynamic current density. However, it remains unclear whether the increase in current density will actually lead to the desired increase in NH_4^+ current efficiency and a decrease in electrochemical energy consumption, because an increase in current density will probably also result in higher concentrations gradients between the base and diluate, leading to more leakage and diffusion. Furthermore, the increase in current density will also increase the applied electric potential, which eventually can lead to a higher electrochemical energy consumption.

Finally, the electric potential can be decreased by lowering the electrical resistance of the BPMED membrane stack by using thinner spacers, which lowered the electrical resistance in reverse electrodialysis (Vermaas et al., 2011).

5. Conclusions

BPMED proved to be able to remove 85–91% of the NH_4^+ from feed water with an initial NH_4^+ concentration of 1.5 g L^{-1} as NH_4HCO_3. The pH in the base was effectively increased from 7.8 to 9.8 and the NH_3 concentration in the base was increased from 0 to 4.5 g L^{-1}. These results show that BPMED can be effectively used to simultaneously remove NH_4^+ from water and produce concentrated dissolved NH_3 in the base. The removal of NH_4^+ from water by BPMED allows for the production of both clean water and NH_3, which can both be reused while avoiding the emission of harmful oxidised nitrogen species and the use of chemicals.

27% of the NH_4^+ transported from the diluate accumulated in the electrode rinse after being transported by electro-migration. Replacing the CEEMs by AEEMs in the BPMED membrane stack prevented the transport to the NH_4^+ to the electrode rinse and therewith the accumulation of NH_4^+ in the electrode rinse. The amount of TAN transported to the base increased to 94%, opening opportunities to produce higher concentrations of NH_3 in the base.

The energy consumption for BPMED remained stable at 19 $MJ \cdot kg\text{-}N^{-1}$, comprising the required energy for the transport of NH_4^+ from the diluate, the dissociation of water for the production of H^+ and OH^- and the pumping energy to recirculate the solutions. The NH_4^+ current efficiency decreased from 69 to 54% throughout the SBEs. The losses in NH_4^+ current efficiency were caused by the leakage of OH^- and the diffusion of dissolved NH_3 and ionic species from the base to the diluate. Because the operational run time and the concentration gradients of OH^-, NH_3 and ionic species between the base and diluate increased throughout the SBEs, the NH_4^+ current efficiency decreased. The electrochemical energy consumption eventually remained stable because the decrease in NH_4^+ current efficiency was compensated by a decrease in electric potential, caused by a decrease in the electrical resistance of the BPMED membrane stack as a result of an increase in the acid and base EC.

Finally, an energetic evaluation showed that the energy consumption of BPMED to remove NH_4^+ and simultaneously produce concentrated dissolved NH_3 was competitive to the combination of ED and addition of chemicals (22 $MJ \cdot kg\text{-}N^{-1}$). With opportunities for further improvements on the efficiency of NH_4^+ transport and in-situ pH change, BPMED makes a good candidate for simultaneous NH_4^+ removal and concentrated dissolved NH_3 production from residual waters.

Author contributions

The manuscript was produced through the contributions of all authors. N. van Linden and G. Bandinu designed and performed the experiments. N. van Linden and G. Bandinu analysed the obtained results in agreement with D.A. Vermaas. H. Spanjers and J.B. van Lier supervised the research. N. van Linden wrote the manuscript and all co-authors provided constructive feedback on the manuscript.

Declaration of competing interest

The authors declare that they have no known competing financial interests or personal relationships that could have appeared to influence the work reported in this paper.

CRediT authorship contribution statement

Niels van Linden: Conceptualization, Methodology, Validation, Investigation, Writing - original draft, Visualization. **Giacomo L. Bandinu:** Conceptualization, Methodology, Investigation. **David A. Vermaas:** Conceptualization, Methodology, Supervision, Writing - review & editing. **Henri Spanjers:** Supervision, Writing - review & editing. **Jules B. van Lier:** Supervision, Writing - review & editing.

Acknowledgements

This study is part of the N2kWh – From Pollutant to Power research (14712), funded by Nederlandse Organisatie voor Wetenschappelijk Onderzoek (NWO) (former Stichting voor de Technische Wetenschappen (STW)) and Agentschap Innoveren & Ondernemen (VLAIO) (former Instituut voor Innovatie door Wetenschap en Technologie (IWT)). We thank the respective funding agencies.

Appendix A. Supplementary data

Supplementary data to this article can be found online at https://doi.org/10.1016/j.jclepro.2020.120788.

References

Ali, M.A.B., Rakib, M., Laborie, S., Viers, P., Durand, G., 2004. Coupling of bipolar membrane electrodialysis and ammonia stripping for direct treatment of wastewaters containing ammonium nitrate. J. Membr. Sci. 244 (1–2), 89–96. https://doi.org/10.1016/j.memsci.2004.07.007.

Cinti, G., Discepoli, G., Sisani, E., Desideri, U., 2016. SOFC operating with ammonia: stack test and system analysis. Int. J. Hydrogen Energy 41 (31), 13583–13590. https://doi.org/10.1016/j.ijhydene.2016.06.070.

El-Bourawi, M.S., Khayet, M., Ma, R., Ding, Z., Li, Z., Zhang, X., 2007. Application of vacuum membrane distillation for ammonia removal. J. Membr. Sci. 301 (1–2), 200–209. https://doi.org/10.1016/j.memsci.2007.06.021.

Erisman, J.W., Bleeker, A., Galloway, J., Sutton, M.S., 2007. Reduced nitrogen in ecology and the environment. Environ. Pollut. 150 (1), 140–149. https://doi.org/10.1016/j.envpol.2007.06.033.

Gineste, J.L., Pourcelly, G., Lorrain, Y., Persin, F., Gavach, C., 1996. Analysis of factors limiting the use of bipolar membranes: a simplified model to determine trends. J. Membr. Sci. 112 (2), 199–208. https://doi.org/10.1016/0376-7388(95)00284-7.

Gonzalez-Martinez, A., Muñoz-Palazon, B., Rodriguez-Sanchez, A., Gonzalez-Lopez, J., 2018. New concepts in anammox processes for wastewater nitrogen removal: recent advances and future prospects. FEMS (Fed. Eur. Microbiol. Soc.) Microbiol. Lett. 365 (6) https://doi.org/10.1093/femsle/fny031.

Graillon, S., Persin, F., Pourcelly, G., Gavach, C., 1996. Development of electrodialysis with bipolar membrane for the treatment of concentrated nitrate effluents. Desalination 107 (2), 159–169. https://doi.org/10.1016/S0011-9164(96)00155-5.

Grasham, O., Dupont, V., Camargo-Valero, M.A., García-Gutiérrez, P., Cockerill, T., 2019. Combined ammonia recovery and solid oxide fuel cell use at wastewater treatment plants for energy and greenhouse gas emission improvements. Appl. Energy 240, 698–708. https://doi.org/10.1016/j.apenergy.2019.02.029.

He, Q., Tu, T., Yan, S., Yang, X., Duke, M., Zhang, Y., Zhao, S., 2018. Relating water vapor transfer to ammonia recovery from biogas slurry by vacuum membrane distillation. Separ. Purif. Technol. 191, 182–191. https://doi.org/10.1016/j.seppur.2017.09.030. Supplement C.

Hong, J., Chen, W., Wang, Y., Xu, C., Xu, X., 2014. Life cycle assessment of caustic soda production: a case study in China. J. Clean. Prod. 66, 113–120. https://doi.org/10.1016/j.jclepro.2013.10.009.

Kampschreur, M.J., Temmink, H., Kleerebezem, R., Jetten, M.S.M., van Loosdrecht, M.C.M., 2009. Nitrous oxide emission during wastewater treatment. Water Res. 43 (17), 4093–4103. https://doi.org/10.1016/j.watres.2009.03.001.

Kuntke, P., Sleutels, T.H.J.A., Rodríguez Arredondo, M., Georg, S., Barbosa, S.G., ter Heijne, A., Hamelers, H.V.M., Buisman, C.J.N., 2018. (Bio)electrochemical ammonia recovery: progress and perspectives. Appl. Microbiol. Biotechnol. 102 (9), 3865–3878. https://doi.org/10.1007/s00253-018-8888-6.

Li, Y., Shi, S., Cao, H., Wu, X., Zhao, Z., Wang, L., 2016. Bipolar membrane electrodialysis for generation of hydrochloric acid and ammonia from simulated ammonium chloride wastewater. Water Res. 89, 201–209. https://doi.org/10.1016/j.watres.2015.11.038. Supplement C.

Lv, Y., Yan, H., Yang, B., Wu, C., Zhang, X., Wang, X., 2018. Bipolar membrane electrodialysis for the recycling of ammonium chloride wastewater: membrane selection and process optimization. Chem. Eng. Res. Des. 138, 105–115. https://doi.org/10.1016/j.cherd.2018.08.014.

Mani, K.N., 1991. Electrodialysis water splitting technology. J. Membr. Sci. 58 (2), 117–138. https://doi.org/10.1016/S0376-7388(00)82450-3.

Mehta, C.M., Khunjar, W.O., Nguyen, V., Tait, S., Batstone, D.J., 2015. Technologies to recover nutrients from waste streams: a critical review. Crit. Rev. Environ. Sci. Technol. 45 (4), 385–427. https://doi.org/10.1080/10643389.2013.866621.

Mondor, M., Masse, L., Ippersiel, D., Lamarche, F., Massé, D.I., 2008. Use of electrodialysis and reverse osmosis for the recovery and concentration of ammonia from swine manure. Bioresour. Technol. 99 (15), 7363–7368. https://doi.org/10.1016/j.biortech.2006.12.039.

Okanishi, T., Okura, K., Srifa, A., Muroyama, H., Matsui, T., Kishimoto, M., Saito, M., Iwai, H., Yoshida, H., Saito, M., Koide, T., Iwai, H., Suzuki, S., Takahashi, Y., Horiuchi, T., Yamasaki, H., Matsumoto, S., Yumoto, S., Kubo, H., Kawahara, J., Okabe, A., Kikkawa, Y., Isomura, T., Eguchi, K., 2017. Comparative study of ammonia-fueled solid oxide fuel cell systems. Fuel Cell. 17 (3), 383–390. https://doi.org/10.1002/fuce.201600165.

PCA, 2016. PCA Ion Exchange Membranes: Technical Data Sheet. PCA GmbH, Heusweiler.

Pronk, W., Biebow, M., Boller, M., 2006. Treatment of source-separated urine by a combination of bipolar electrodialysis and a gas transfer membrane. Water Sci. Technol. 53 (3), 139–146.

Saadabadi, S.A., Thallam Thattai, A., Fan, L., Lindeboom, R.E.F., Spanjers, H., Aravind, P.V., 2019. Solid oxide fuel cells fuelled with biogas: potential and constraints. Renew. Energy 134, 194–214. https://doi.org/10.1016/j.renene.2018.11.028.

Sander, R., 2015. Compilation of Henry's law constants (version 4.0) for water as solvent. Atmos. Chem. Phys. 15 (8), 4399–4981. https://doi.org/10.5194/acp-15-4399-2015.

Shi, L., Hu, Y., Xie, S., Wu, G., Hu, Z., Zhan, X., 2018. Recovery of nutrients and volatile fatty acids from pig manure hydrolysate using two-stage bipolar membrane electrodialysis. Chem. Eng. J. 334, 134–142. https://doi.org/10.1016/j.cej.2017.10.010.

Shuangchen, M., Tingting, H., Lan, M., Jingxiang, M., Gongda, C., Jing, Y., 2015. Experimental study on desorption of simulated solution after ammonia carbon capture using bipolar membrane electrodialysis. Int. J. Greenh. Gas Control 42, 690–698. https://doi.org/10.1016/j.ijggc.2015.09.020.

Staniforth, J., Ormerod, R.M., 2003. Clean destruction of waste ammonia with consummate production of electrical power within a solid oxide fuel cell system. Green Chem. 5 (5), 606–609. https://doi.org/10.1039/B307396N.

Strathmann, H., 2004. Chapter 4 - Operating Principle of Electrodialysis and Related Processes *Ion-Exchange Membrane Separation Processes*, 9 ed. Elsevier, pp. 147–225.

Strathmann, H., 2010. Electrodialysis, a mature technology with a multitude of new applications. Desalination 264 (3), 268–288. https://doi.org/10.1016/j.desal.2010.04.069.

Tongwen, X., 2002. Electrodialysis processes with bipolar membranes (EDBM) in environmental protection—a review. Resour. Conserv. Recycl. 37 (1), 1–22. https://doi.org/10.1016/S0921-3449(02)00032-0.

van Linden, N., Spanjers, H., van Lier, J.B., 2019. Application of dynamic current density for increased concentration factors and reduced energy consumption for concentrating ammonium by electrodialysis. Water Res., 114856 https://doi.org/10.1016/j.watres.2019.114856.

Vermaas, D.A., Saakes, M., Nijmeijer, K., 2011. Doubled power density from salinity gradients at reduced intermembrane distance. Environ. Sci. Technol. 45 (16), 7089–7095. https://doi.org/10.1021/es2012758.

Ward, A.J., Arola, K., Thompson Brewster, E., Mehta, C.M., Batstone, D.J., 2018. Nutrient recovery from wastewater through pilot scale electrodialysis. Water Res. 135, 57–65. https://doi.org/10.1016/j.watres.2018.02.021.

Xie, M., Shon, H.K., Gray, S.R., Elimelech, M., 2016. Membrane-based processes for wastewater nutrient recovery: technology, challenges, and future direction. Water Res. 89, 210–221. https://doi.org/10.1016/j.watres.2015.11.045.